Published in final edited form as:
Microw Opt Technol Lett. 2011 August ; 53(8): 1896–1902. doi:10.1002/mop.26128.

Heterogeneous Anthropomorphic Phantoms with Realistic Dielectric Properties for Microwave Breast Imaging Experiments

Alireza Mashal, **Fuqiang Gao**, and **Susan C. Hagness**
Department of Electrical and Computer Engineering, University of Wisconsin, Madison, WI, 53706 USA

Alireza Mashal: amashal@gmail.com; Fuqiang Gao: fgao4@wisc.edu; Susan C. Hagness: hagness@engr.wisc.edu

Abstract

We present a technique for fabricating realistic breast phantoms for microwave imaging experiments. Using oil-in-gelatin dispersions that mimic breast tissue dielectric properties at microwave frequencies, we constructed four heterogeneous phantoms spanning the full range of volumetric breast densities. We performed CT scans and dielectric properties measurements to characterize each phantom.

Keywords

microwave imaging; breast phantoms; dielectric spectroscopy

1. INTRODUCTION

Microwave breast imaging is a non-ionizing molecular imaging technique that senses the endogenous -- and possibly exogenously influenced -- dielectric properties of breast tissue. Microwave imaging shows much promise as a safe, low-cost, three-dimensional tomographic imaging modality. Potential applications include early-stage breast cancer detection, breast density evaluation, and cancer treatment monitoring. Definitive, quantitative validation of microwave imaging techniques is a critical component in the development of this technology. Clinical studies with human subjects provide the ultimate test domain but also pose the most challenging validation scenario due to the fact that the true *in vivo* properties are not known. This emphasizes the important role of realistic physical phantoms in pre-clinical validation studies. Phantoms have the potential to provide an anthropomorphic test domain with known structure and known dielectric properties that reasonably mimic tissue in the breast.

Table 1 summarizes the features of numerous breast phantoms that have been reported over the past decade. The shape and structural complexity of the phantoms vary considerably, ranging from simple geometrically defined volumes with predominantly homogeneous interiors to realistically shaped volumes with heterogeneous interiors. The materials in these phantoms range from those with dielectric properties which roughly approximate breast tissue properties at select frequencies to tissue-mimicking (TM) materials [1] that closely match the dielectric properties of certain tissues in the breast over a wide frequency range. However, none of the phantoms reported to date include fibroglandular mimicking materials with properties that match those reported in the large-scale Wisconsin-Calgary study of breast tissue [2].

fax: 608-262-1267.

Our present investigation is motivated not only by the need for individual realistic breast phantoms that accurately model the shape, structural complexity, and microwave-frequency dielectric properties of fatty and fibroglandular tissue in the human breast, but also by the need for sets of realistic breast phantoms that span the full range of volumetric breast densities observed in the general patient population. Breast density refers to the percentage of fibroglandular tissue in the breast. High breast density is one of the strongest predictors of breast cancer risk [3] and also impedes mammographic screening [4]. Accordingly, it is of great interest and importance to evaluate the performance of microwave imaging across the full range of breast densities.

In this paper, we present a method for constructing stable, heterogeneous anthropomorphic breast phantoms with realistic dielectric properties. We illustrate the approach by constructing four phantoms with different breast densities. We select oil-in-gelatin TM materials that accurately model the dielectric properties of skin, fat, and fibroglandular breast tissues. The percentage of fibroglandular TM material is varied to create low and high breast density phantoms. CT images of the completed phantoms are obtained to confirm the interior spatial distribution of the various TM materials. We confirm the integrity of the dielectric properties distribution by cutting each breast phantom in half and conducting direct dielectric-properties measurements of the different regions of the interior.

The remainder of this paper is organized as follows. In Section 2 we discuss the TM materials employed in constructing the phantoms, the phantom construction method, and dielectric measurement techniques. In Section 3 we report the measured dielectric properties and CT-imaged structural composition of the constructed phantoms. Our conclusions are presented in Section 4.

2. MATERIALS AND METHODS

2.1 Design of tissue-mimicking materials

We created the TM materials from oil-in-gelatin dispersions reported by [1]. The TM materials are composed of water, gelatin, oil (1:1 mixture of kerosene and safflower oil), and preservatives. Varying the concentration of oil alters the dielectric properties. Higher oil concentrations result in materials with dielectric properties that are similar to those of lower-water-content tissue, while lower oil concentrations result in materials that mimic higher water-content tissues. These materials are relatively inexpensive to fabricate, can conform to any shape, and have stable dielectric properties even when placed in direct contact with other TM materials. In addition, the fabrication procedure may be altered to allow for the inclusion of contrast agents, such as carbon nanotubes [14].

The TM materials in our breast phantoms were designed to achieve a close match to the breast tissue properties reported in [2] and wet and dry skin properties reported in [15]. [2] categorized breast tissue into three different groups based on adipose composition; hereafter we refer to these groups as fibroglandular (0–30% adipose), heterogeneous mix (31–84% adipose), and fat (85–100% adipose). We designed one or two TM materials for each of these groups of breast tissue, and one TM material for skin. An even greater level of dielectric heterogeneity in the phantom may be achieved by designing two or more distinct TM materials (e.g., with different oil concentrations) for each breast tissue group.

2.2 Dielectric characterization of tissue-mimicking materials

We conducted two sets of dielectric characterization measurements. The purpose of the first set was to design the TM materials, as described above. The purpose of the second set was twofold: 1) to investigate the within-sample variability of the dielectric properties of a given TM material, and 2) to investigate the stability of the dielectric properties of each TM

material when placed in contact with other TM materials, in an environment similar to that of the constructed phantom. A portion of each TM material fabricated during the phantom construction phase of this study was set aside for the second set of experiments.

Two multi-layer cylindrical test volumes were constructed, each from a different batch of the TM materials, as follows. A 1-cm-thick layer of the skin-mimicking material was poured into a 10-cm-diameter cylindrical container and allowed to congeal. Layers of 4-cm-thick fat-, heterogeneous-mix-, and fibroglandular-mimicking materials were added one-by-one in a similar manner, yielding a 13-cm-high test volume. After one week, each test volume was removed from its cylindrical container and the layers were separated. We note that the ease of separation served as one indication that no osmosis had occurred between adjacent layers.

We measured the dielectric properties at three different locations on each surface (top and bottom) of each TM material layer from each of the two test volumes. Thus we obtained dielectric properties data from a total of 12 measurement sites for each TM material. The dielectric measurements were conducted using the wideband open-ended coaxial probe technique described in [16].

2.3 Phantom construction

Each breast phantom was constructed in three stages using an outer and inner mold. The outer mold (~ 400 mL volume) was shaped similar to the human breast in a prone position; identical outer molds were used for all four phantoms. The inner mold was unique to each phantom as it was used to control the volume of the heterogeneous mix and fibroglandular content in relation to the fat content. In addition, the inner mold was configured to provide a unique structurally complex interface between the fat and fibroglandular regions.

In the first stage of phantom construction, we created a thin skin layer (1–2 mm) on the inner surface of the outer mold by pouring a small amount of the skin-mimicking material into the outer mold in its liquid state and rotating the mold as the TM material cooled and congealed on the inner surface of the mold. The skin-mimicking material was also used to create a slightly thicker layer at the anterior end of the mold. This feature provided a reasonably good model of the areola. The skin layer was allowed to fully congeal for 5 hours before proceeding to the next stage.

In the second stage, the fat layer was added on the top of the skin layer. This was accomplished by suspending the inner mold inside the outer mold and pouring the fat-mimicking material into the space between the inner and outer molds. The volume of each inner mold was chosen to achieve a representative breast density for that phantom class. For example, for a class I phantom (mostly fat), the volume of the heterogeneous mix and fibroglandular content was chosen to be approximately 10% of the total breast volume. Similarly we chose inner-mold volumes to be approximately 30%, 50%, and 70% of the total breast volume to construct class II (scattered fibroglandular), class III (heterogeneously dense), and class IV (extremely dense) phantoms, respectively.

In the final stage, after allowing the fat layer to congeal for 12 hours, the heterogeneous-mix-mimicking material was added to the void left by the removal of the inner mold. Randomly shaped pieces of already congealed fibroglandular-mimicking materials were added to the heterogeneous mix as it was poured. Once the phantom was completed, it was covered by a thin sheet of polyethylene material and allowed to set for approximately one week before it was removed from the outer mold.

3. RESULTS AND DISCUSSION

3.1 Dielectric properties characterization of TM materials

The dielectric properties of the TM materials used for the construction of the four different phantoms are shown in Figures 1 and 2. In these figures, each curve with vertical bars represents the average properties (relative permittivity or effective conductivity) of 12 measurements made on the different cylindrical TM samples described in Section 2.2. The vertical bars span the maximum and minimum values at specific frequencies. The small variability across measurements of each TM material demonstrate the spatial uniformity and stability of the dielectric properties of the TM materials even when placed in contact with TM materials of different oil concentrations.

We used 20% and 30% -oil TM materials to represent fibroglandular tissue, 40%-oil to represent the heterogeneous mix, and 80%-oil to represent fat. Figure 1 shows that these TM materials closely mimic the dielectric properties of the corresponding breast tissue types reported in [2] across the 1–6 GHz frequency range. For all the breast tissue types, the dielectric properties of the TM materials fall within the range of the 25th and 75th percentile of the breast tissue group they represent.

A 30%-oil TM material was chosen to represent skin tissue. Figure 2 shows the dielectric properties of wet and dry skin tissue types [15] and 30%-oil TM material. The relative permittivity of the skin-mimicking material falls between that of wet and dry skin in the 1–6 GHz frequency range. The effective conductivity of the skin-mimicking material is slightly higher than that of wet skin. This small discrepancy in conductivity should have a negligible effect on microwave scattering since the skin layer is only 1–2 mm thick.

3.2 Phantom characterization

Figure 3 shows a photograph of one of the four completed phantoms after the outer mold has been removed. The height of the phantom is approximately 8 cm. The diameter at the base is approximately 12 cm. A CT scan of each of the four phantoms was acquired approximately one week after construction. Figure 4 shows a sagittal and coronal CT image of a central cross-section of each phantom. These images confirm the integrity of each of the spatial features of the phantoms. For each phantom, the CT images clearly show the presence of skin and areola (medium grey), fat (black), heterogeneous mix (medium grey), and fibroglandular tissue (light grey). In addition, the CT images show the variations in fibroglandular tissue density across the four different phantoms. The small dark circles in the images are air bubbles (typically less than 1 mm in diameter) that are introduced unintentionally during fabrication of the TM materials. The dielectric properties of the various TM materials inside the phantom were verified by making a coronal cross-sectional cut through each phantom and making measurements at approximately 1 cm intervals along a trans-sectional line across the exposed coronal plane. Figures 5(a),(b) and 6(a),(b) show the dielectric properties in the 1–6 GHz range at various trans-sectional positions for the class I and class IV phantoms. This data confirms that a large dielectric contrast (>5:1 in some cases) between fatty and fibroglandular content is present, as desired. Parts (c) and (d) of Figures 5 and 6 show the dielectric properties of the phantoms at 3 GHz as a function of position. These graphs provide a spatial snapshot of the interior heterogeneity as well as the increasing fibroglandular density with phantom class number. For example, a comparison of Figures 5(c),(d) and Figures 6(c),(d) shows that there is significantly more higher-water-content TM material in the class IV phantom (extremely dense) than the class I phantom (mostly fat), as desired.

These phantoms are well suited for experimental imaging tests. The phantoms are relatively sturdy and are not easily damaged during gentle handling. In addition, the TM materials

used to construct these phantoms have been shown to be stable over a nine-week period as long as they are not exposed to air for long periods of time [1]. The TM materials are also stable in oil (1:1 mixture of kerosene and safflower oil); this is an important feature for experiments that require the phantoms to be immersed in a coupling medium.

4. CONCLUSIONS

We have described the construction of four different realistic breast phantoms, each representing a different volumetric breast density classification. The phantoms were constructed using TM materials that accurately represent the dielectric properties of various breast tissues. The phantoms were heterogeneous, each with a skin layer and a complex network of fibroglandular and fatty tissues. We verified the integrity of the internal structure of the phantom by obtaining CT images. The dielectric properties of the phantom constituents were verified by cutting the phantoms in half and measuring the dielectric properties of the phantom cross-section. These phantoms were constructed using simple techniques and have long term stability when not exposed to air for long periods of time. The techniques described here may be easily modified to construct phantoms with malignant lesions.

Acknowledgments

The authors would like to thank Christine Jaskowiak (University of Wisconsin, School of Medicine and Public Health) for her assistance in obtaining the CT images. This work was supported by the Department of Defense Breast Cancer Research Program under grant W81XWH-07-1-0629 and the National Institutes of Health under grant R01CA112398 awarded by the National Cancer Institute.

REFERENCES

1. Lazebnik M, Madsen EL, Frank GR, Hagness SC. Tissue-mimicking phantom materials for narrowband and ultrawideband microwave applications. Physics in Medicine and Biology. 2005; 50(no. 18):4245–4258. [PubMed: 16148391]
2. Lazebnik M, McCartney L, Popovic D, Watkins CB, Lindstrom MJ, Harter J, Sewall S, Magliocco A, Booske JH, Okoniewski M, Hagness SC. A large-scale study of the ultrawideband microwave dielectric properties of normal breast tissue obtained from reduction surgeries. Physics in Medicine and Biology. 2007; 52(no. 10):2637–2656. [PubMed: 17473342]
3. Kerlikowske K, Ichikawa L, Miglioretti DL, Buist DSM, Vacek PM, Smith-Bindman R, Yankaskas B, Carney PA, Ballard-Barbash R. Longitudinal measurement of clinical mammographic breast density to improve estimation of breast cancer risk. Journal of the National Cancer Institute. 2007; 99(no. 5):386–395. [PubMed: 17341730]
4. Carney PA, Miglioretti DL, Yankaskas BC, Kerlikowske K, Rosenberg R, Rutter CM. Individual and combined effects of age, breast density, and hormone replacement therapy use on the accuracy of screening mammography. Annals of Internal Medicine. 2003; 138(no. 3):168–175. [PubMed: 12558355]
5. Meaney PM, Yagnamurthy NK, Paulsen KD. Pre-scaled two-parameter Gauss-Newton image reconstruction to reduce property recovery imbalance. Physics in Medicine and Biology. 2002; 47(no. 7):1101–1119. [PubMed: 11996058]
6. Li D, Meaney PM, Tosteson TD, Jiang S, Kerner TE, McBride TO, Pogue BW, Hartov A, Paulsen KD. Comparisons of three alternative breast modalities in a common phantom imaging experiment. Medical Physics. 2003; 30(no. 8):2194–2205. [PubMed: 12945985]
7. Sill JM, Fear EC. Tissue sensing adaptive radar for breast cancer detection – experimental investigation of simple tumor models. IEEE Transactions on Microwave Theory and Techniques. 2005; 53(no. 11):3312–3319.
8. Winters DW, Shea JD, Madsen EL, Frank GR, Van Veen BD, Hagness SC. Estimating the breast surface using UWB microwave monostatic backscatter measurements. IEEE Transactions on Biomedical Engineering. 2008 no. 1.55:247–256. [PubMed: 18232368]

9. Klemm M, Leendertz JA, Gibbins D, Craddock IJ, Preece A, Benjamin R. Microwave radar-based breast cancer detection: Imaging in inhomogeneous breast phantoms. IEEE Antennas and Wireless Propagation Letters. 2009; 8:1349–1352.

10. Salvador SM, Vecchi G. Experimental tests of microwave breast cancer detection on phantoms. IEEE Transactions on Antennas and Propagation. 2009; 57(no. 6):1705–1712.

11. Miyakawa M, Takata S, Inotsume K. Development of non-uniform breast phantom and its microwave imaging for tumor detection by CP-MCT. Proceedings of the Annual International Conference of the IEEE Engineering in Medicine and Biology Society. 2009:2723–2726.

12. Croteau J, Sill J, Williams T, Fear E. Phantoms for testing radar-based microwave breast imaging. 13th International Symposium on Antenna Technology and Applied Electromagnetics and Canadian Radio Sciences Meeting. 2009

13. Ostadrahimi M, Reopelle R, Noghanian S, Pistorius S, Vahedi A, Safari F. A heterogeneous breast phantom for microwave breast imaging. Proceedings of the Annual International Conference of the IEEE Engineering in Medicine and Biology Society. 2009:2727–2730.

14. Mashal A, Sitharaman B, Li X, Avti PK, Sahakian AV, Booske JH, Hagness SC. Toward carbon-nanotube-based theranostic agents for microwave detection and treatment of breast cancer: Enhanced dielectric and heating response of tissue-mimicking materials. IEEE Transactions on Biomedical Engineering. 2010; 57(no. 8):1831–1834. [PubMed: 20176534]

15. Gabriel S, Lau RW, Gabriel C. The dielectric properties of biological tissues: III. Parametric models for the dielectric spectrum of tissues. Physics in Medicine and Biology. 1996; 41(no. 11): 2271–2293. [PubMed: 8938026]

16. Popovic D, McCartney L, Beasley C, Lazebnik M, Okoniewski M, Hagness SC, Booske JH. Precision open-ended coaxial probes for in vivo and ex vivo dielectric spectroscopy of biological tissues at microwave frequencies. IEEE Transactions on Microwave Theory and Techniques. 2005; 53(no. 5):1713–1722.

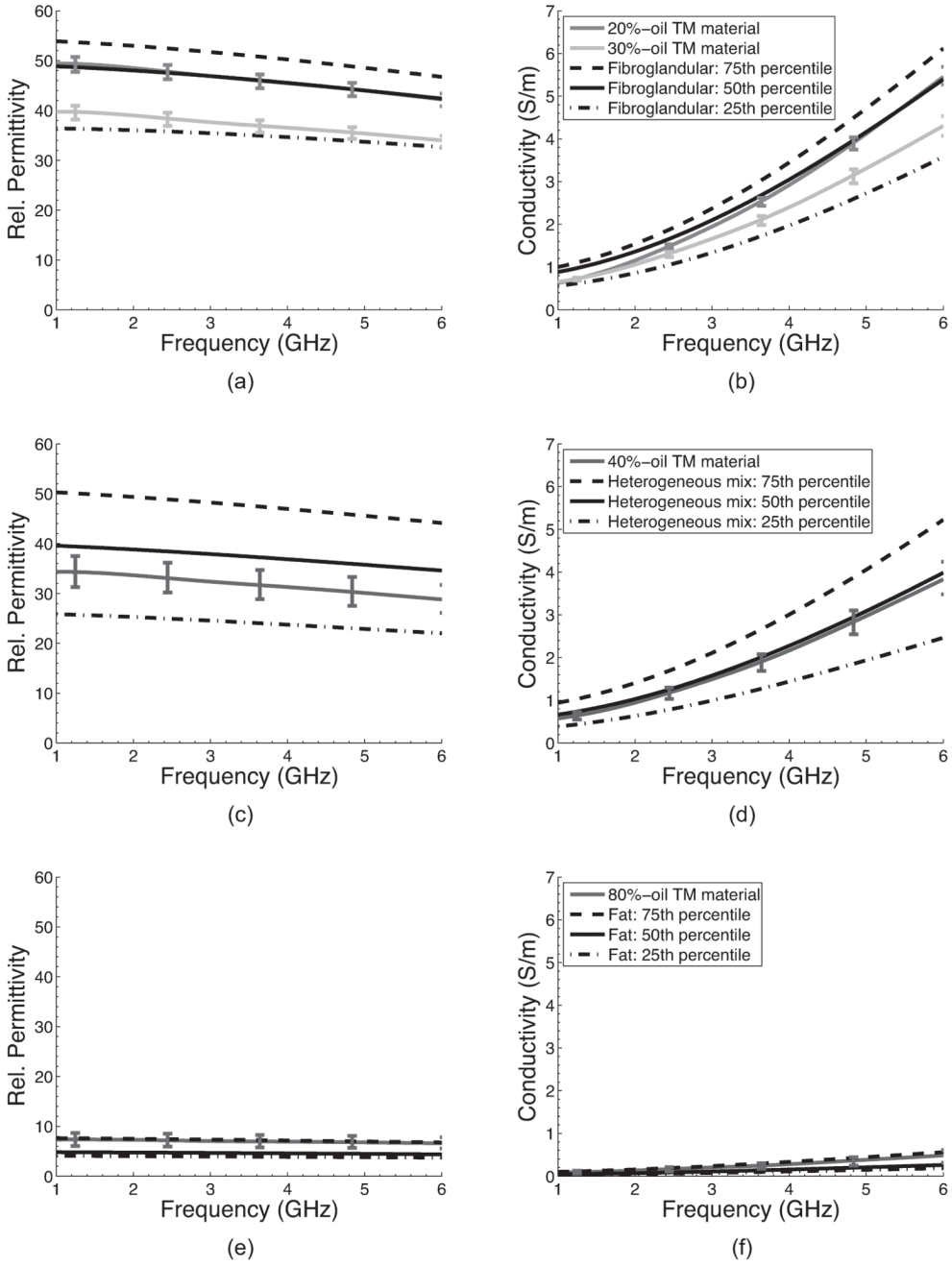

Figure 1.

Comparison of the dielectric properties of (a)–(b) fibroglandular, (c)–(d) heterogeneous mix (both fibroglandular and fatty tissue), and (e)–(f) fatty tissue and the TM materials used to construct the four different breast phantoms. The curves without vertical bars are the 75th (dashed lines), 50th (solid lines), and 25th (dash-dotted lines) percentile breast tissue data reported in [2]. The solid curves with vertical bars are the average of 12 dielectric properties measurements made on two TM material samples with the specified concentration of oil; the vertical bars span the maximum and minimum property values at specific frequencies.

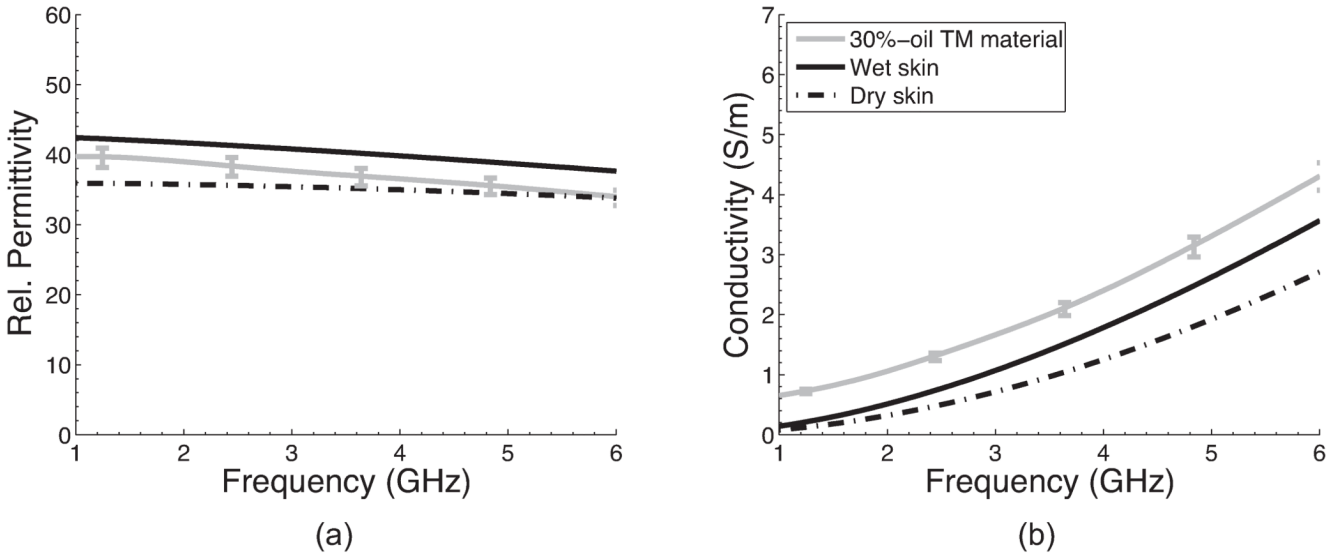

Figure 2.

Comparison of the dielectric properties of wet and dry skin [15] and the 30%-oil TM material. The solid curve with vertical bars is the average of 12 dielectric properties measurement made on two 30%-oil TM material samples; the vertical bars span the maximum and minimum property values at specific frequencies.

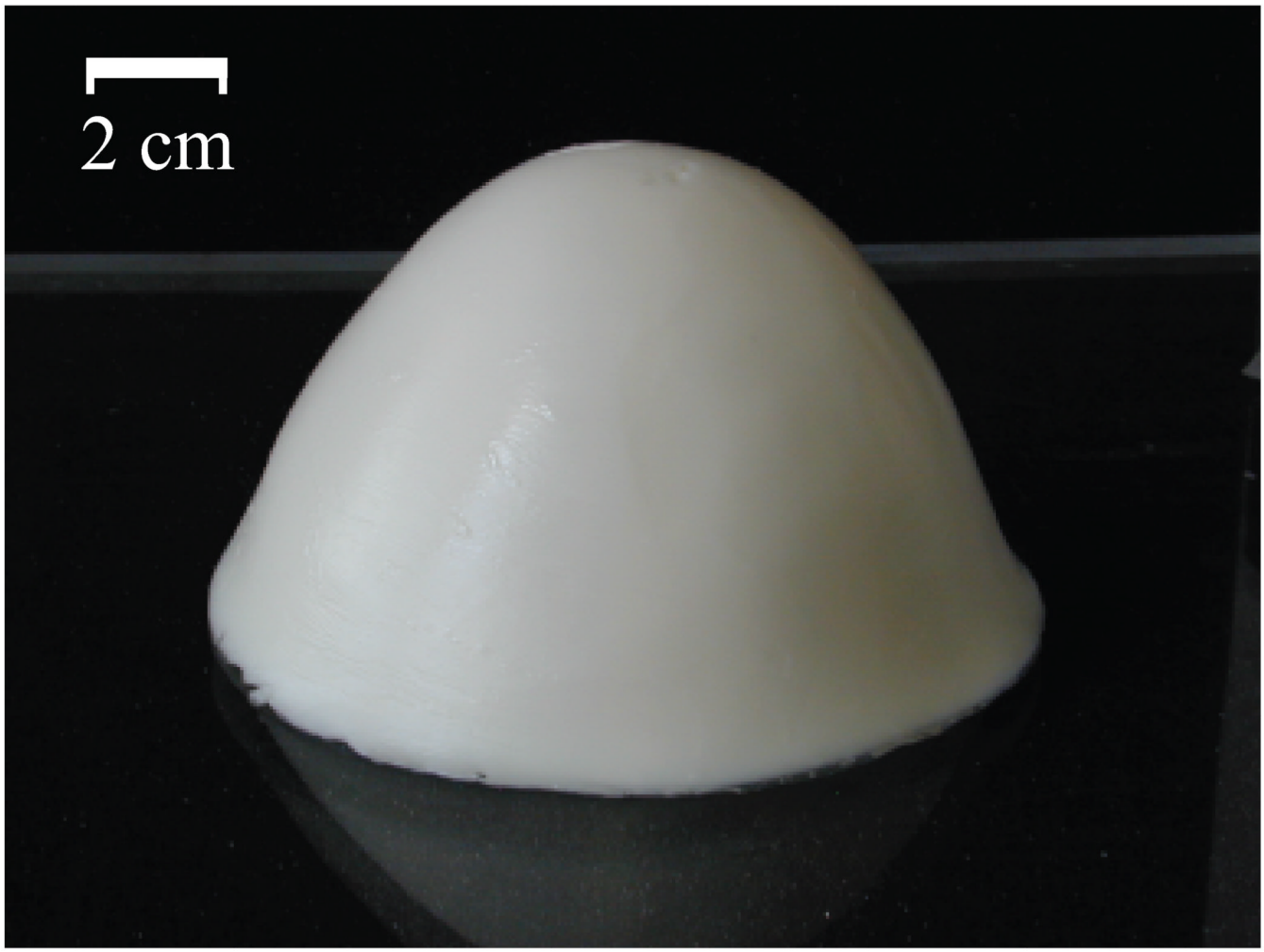

Figure 3.
Photograph of a breast phantom after construction.

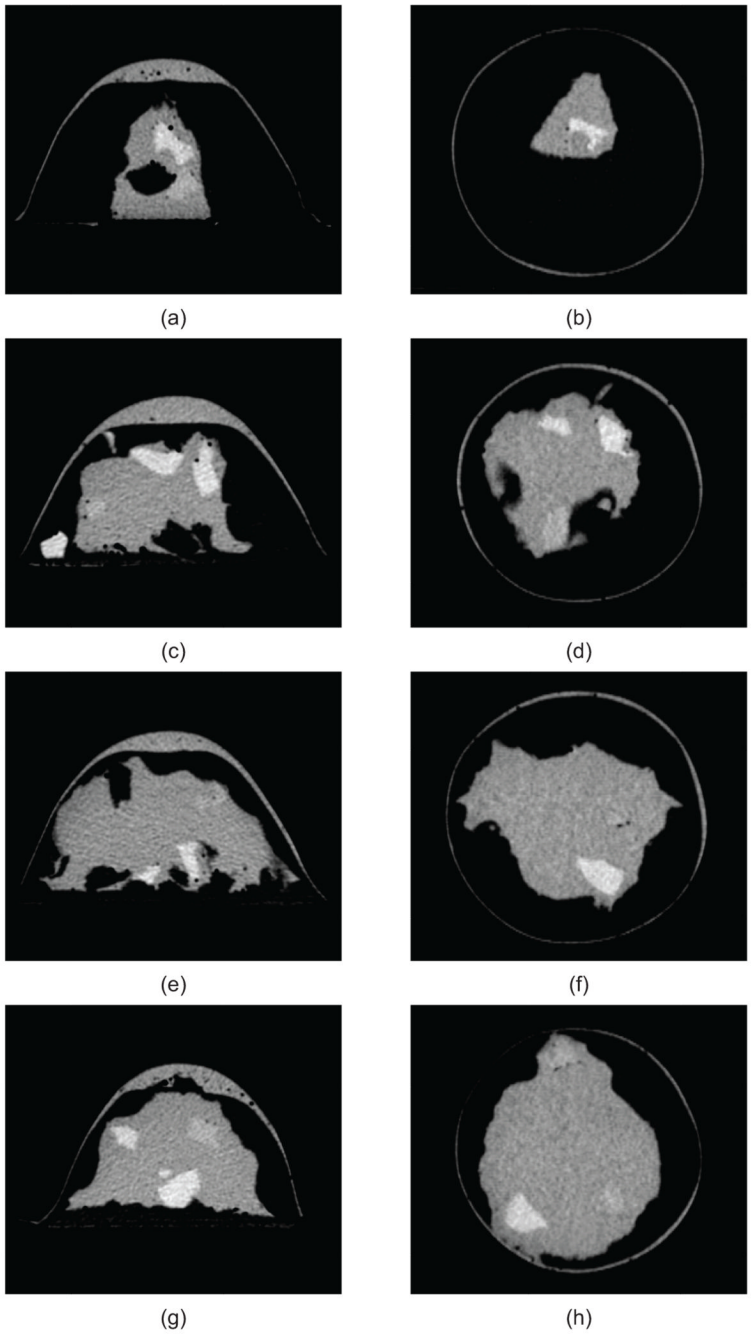

Figure 4.
CT images of sagittal (left) and coronal (right) cross-sections of four phantoms: (a)–(b) class I (mostly fat), (c)–(d) class II (scattered fibroglandular), (e)–(f) class III (heterogeneously dense), and (g)–(h) class IV (extremely dense). Features present in each phantom include a skin layer and areola (medium grey), fat (black), heterogeneous mix (medium grey), and fibroglandular (light grey) tissue.

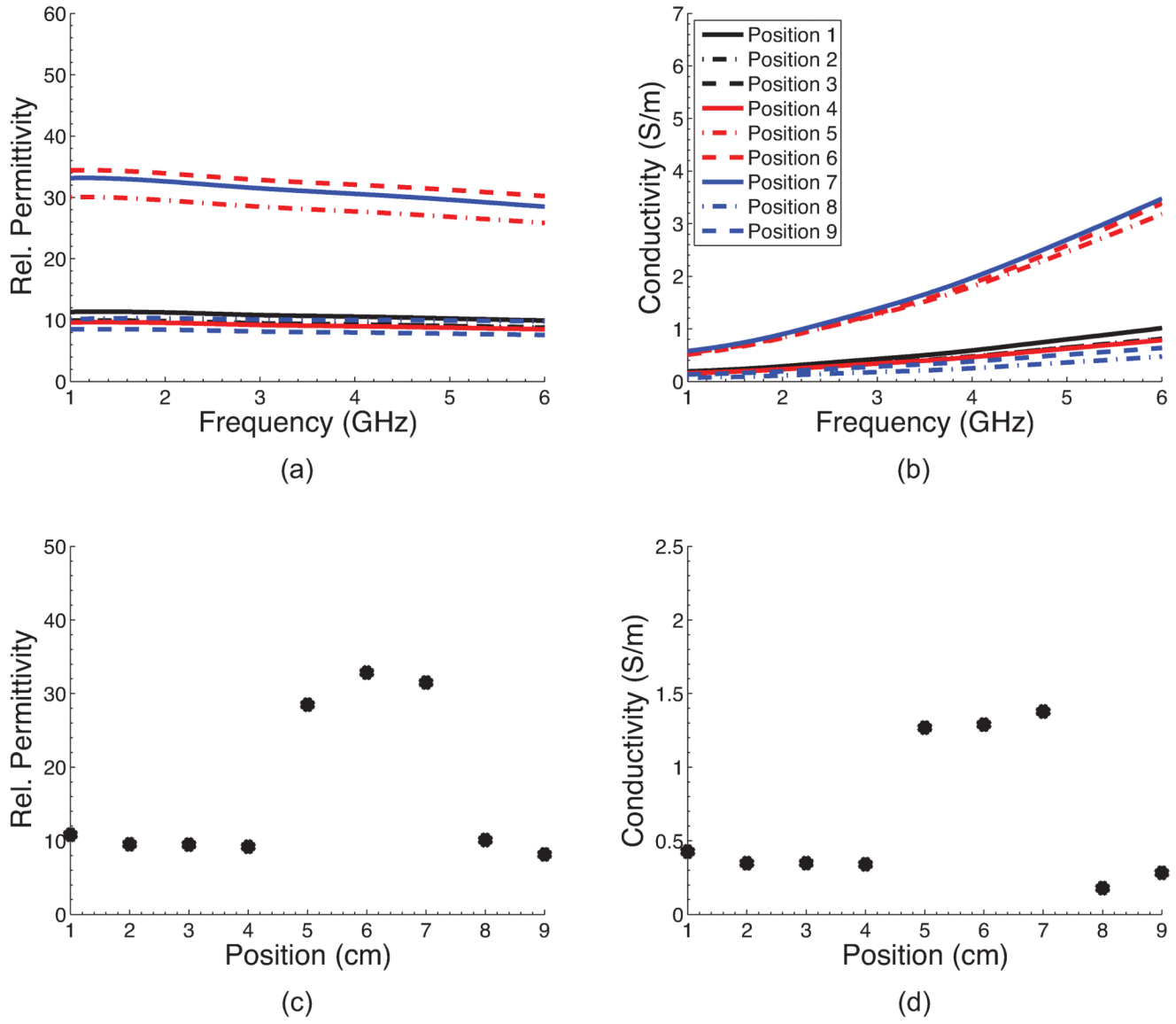

Figure 5.
Dielectric properties at nine positions along an interior trans-sectional line through the class I phantom. (a)–(b) Dielectric properties across the 1–6 GHz frequency range. (c)–(d) Dielectric properties at 3 GHz as a function of position.

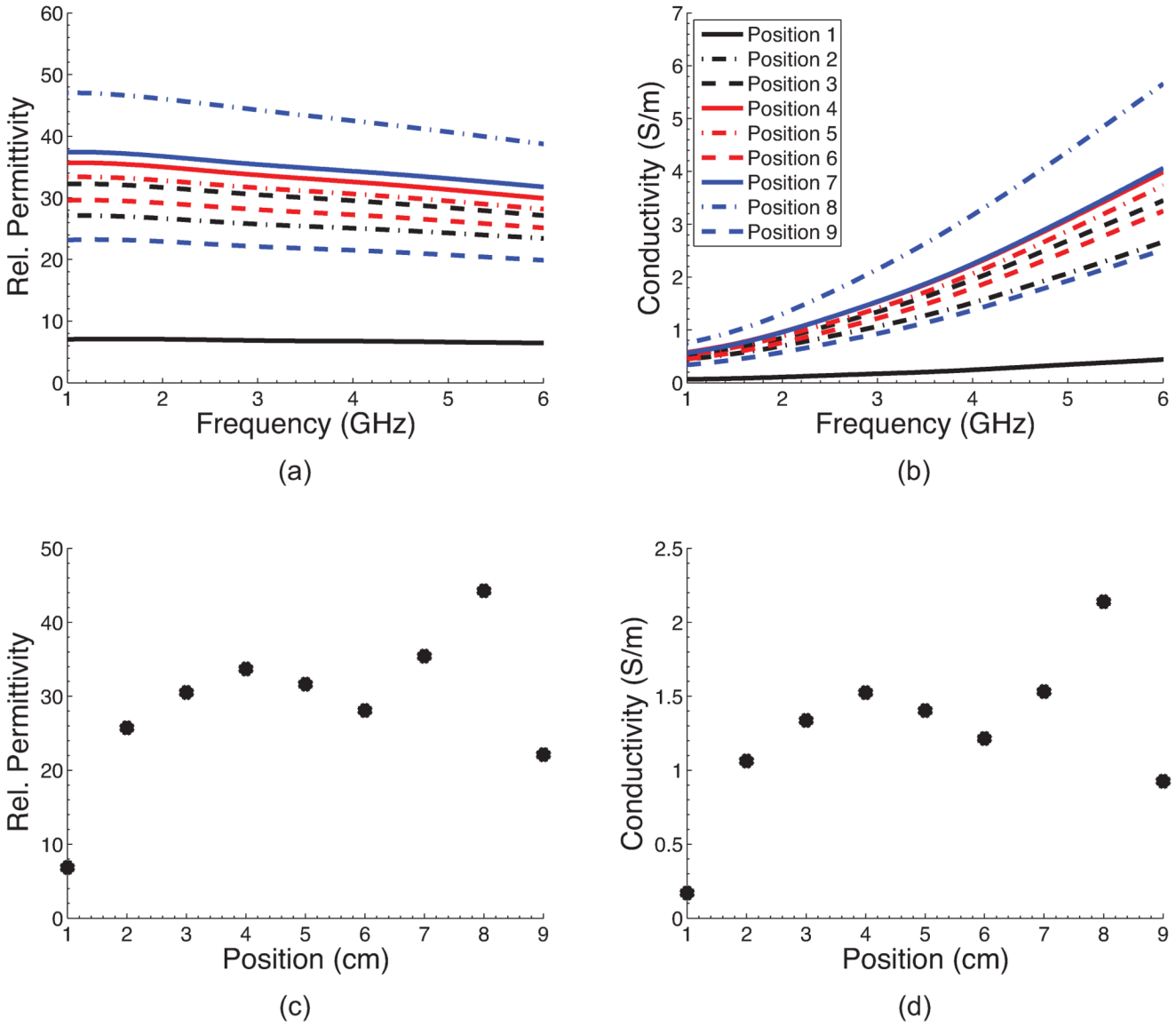

Figure 6.

Dielectric properties at nine positions along an interior trans-sectional line through the class IV phantom. (a)–(b) Dielectric properties across the 1–6 GHz frequency range. (c)–(d) Dielectric properties at 3 GHz as a function of position.

Microw Opt Technol Lett. Author manuscript; available in PMC 2011 August 22.

TABLE 1

Summary of Previously Published Work on Breast Phantoms for Microwave Imaging Applications

Materials used for construction	Breast shape	ε_r, σ(S/m) of constituents				Frequency (GHz)	Citation
		Skin	Fat	Fibroglandular	Tumor		
Corn syrup, NaCl, agar	Cylinder			ε_r=23 σ=0.2	ε_r=53.5 σ=1.2	1.35	[5]
Corn syrup, agar	Cylinder			ε_r=42 σ=0.67	ε_r=74 σ=1.6	0.9	[6]
Silicone sheet dough, alginate	Cylinder	ε_r ~ 34.3 σ=2–4	ε_r=4.5–4 σ=0.06–0.2		ε_r ~ 43.7 σ=5–8	1–7	[7]
Oil-in-gelatin	Realistic	ε_r=40–30 σ=0.6–10.5	ε_r=8–7.1 σ=0.05–1.1			1–11	[8]
Liquid, gelatin, polythene	Hemisphere	ε_r=35 σ NA	ε_r=10 σ NA	ε_r=27 σ NA	ε_r=50 σ NA	3	[9]
Dough, water	Truncated cone			ε_r=80–64 σ=0.1–15	ε_r=50–27 σ=0.1–9	1–9	[10]
Isoparaffin, salt, sugar, water	Realistic	ε_r=40.8 σ=1.79	ε_r=5.3 σ=0.13			2.5	[11]
Oil-in-gelatin	Realistic	ε_r=34–21 σ=0.5–10	ε_r=7.5–5.5 σ=0.01–1.8	ε_r=25–22.5 σ=0.5–10	ε_r=47.5–30 σ=0.5–015	0.05–13.51	[12]
Oil-in-gelatin	Cylinder	ε_r=46–35 σ=12.5–18	ε_r=5–4.5 σ ~ 1	ε_r=26–20 σ=2.5–5	ε_r=55–40 σ=15–21	0.5–8	[13]

Blank entry: Phantom did not have listed constituent.

NA: Not available (phantom included listed constituent, but the dielectric properties were not reported).